

Waterproof Soft Robot Hand with Variable Stiffness Wire-driven Finger Mechanism Using Low Melting Point Alloy for Contact Pressure Distribution and Concentration

Toshinori Hirose, Shingo Kitagawa, Shun Hasegawa, Yohei Kakiuchi, Kei Okada and Masayuki Inaba¹

Abstract— We have proposed a soft flexible wire-driven finger mechanism with a soft skin and two coil springs. This finger mechanism has many joints on a narrow pitch, and good at distributing the contact pressure and following various object shapes, especially during human contact motions such as massage. But it is difficult to concentrate the contact pressure on the fingertips for pinching a small object or acupressure on the human body. Therefore, in this paper, we propose the various stiffness wire-driven finger mechanism, which is a fusion of the conventional finger mechanism and a new various stiffness unit. This makes it possible to selectively change the stiffness of the variable stiffness unit, change the flexibility of the joints near the fingertip, and switch between distribution and concentration of contact pressure. The various stiffness unit is a tube containing a low melting point alloy (LMPA). A LMPA has the advantages of high tensile strength at high stiffness, and easy realization of a waterproof and compact structure compared to other methods such as powder jamming, ER fluid, MR fluid, and shape memory polymers (SMP). We also developed a waterproof soft robot hand using this finger mechanism and conducted massage and hair washing experiments by remote control.

I. INTRODUCTION

In recent years, with the progress of aging in Japan, the demand for massage for the purpose of recovering the physical function deteriorated due to aging is increasing in the medical or nursing field. In addition, with the sophistication and complexity of modern society, the number of people suffering from mental illness such as depression and stress is increasing, and the demand for massage and hair washing (scalp massage) for the purpose of healing and relaxation is also increasing.

At the same time, the birthrate is declining and the shortage of the working population is regarded as a problem, and it is thought that the need for automation will increase in fields such as massage and hair washing that provide care by contacting the human body. In addition, in the case of a global pandemic such as the recent new coronavirus infection, it is necessary to avoid contact between people, and there is a growing need for automation temporarily.

In the automation of human contact motions such as massage and hair washing, the generated contact pressure itself is very important. Excessive concentration of contact pressure may cause discomfort to the person, cause poor

¹Toshinori Hirose, Shingo Kitagawa, Shun Hasegawa, Yohei Kakiuchi, Kei Okada and Masayuki Inaba are with Department of Mechano-Informatics, Graduate School of Information Science and Technology, The University of Tokyo, 7-3-1 Hongo, Bunkyo-ku, Tokyo 113-8656, Japan
hirose@jsk.t.u-tokyo.ac.jp

blood circulation, and cause harm to the person. In particular, unlike the contact motion with an artificial object, the shape and size of the human body part differs person to person, so the robot hand is required to follow various contact objects and distribute the contact pressure.

But in the human contact motions where contact pressure should be concentrated, if the contact pressure is distributed more than necessary, it is not possible to loosen muscles to improve blood circulation or stimulate nerves to provide healing effects. On the contrary, the acupressure is one of the motion in which the contact pressure must be concentrated, and it is necessary to properly use the distribution and concentration of the contact pressure in the human contact motion.

In addition to human contact motion, for example, when gripping agricultural products and artificial objects, it is required to distribute the contact pressure and grip the object without damaging it. On the other hand, when gripping a small object, the pinching motion may be suitable, and it is necessary to properly use the distribution and concentration of the contact pressure according to the object.

In this paper, we decided to develop a robot hand that achieves both distribution and concentration of contact pressure. We took an approach of considering a soft flexible structure that realizes the distribution of contact pressure first, and then adding more elements to the structure to selectively change the stiffness to realize both the distribution and concentration of contact pressure. The developed robot hand is also waterproof for use in watery environments such as washing hair, and for cleaning itself with water or disinfecting itself with alcohol.

II. COMPATIBILITY BETWEEN CONTACT PRESSURE DISTRIBUTION AND CONCENTRATION

The soft flexible wire-driven finger mechanism with a soft skin[1], which we have proposed so far, realizes contact pressure distribution and was good at generating compound pressure over the entire finger. There was a problem that it was difficult to concentrate the tendon on the fingertip and generate a single point pressure. Therefore, we investigated a method of concentrating contact pressure on the fingertips.

As a method of concentrating the contact pressure on the fingertip, there is a method of increasing the number of actuators and controlling them independently, but this is not desirable because the compactness is impaired. So, instead of

increasing the number of actuators, we focused on a method of changing the flexibility by changing the stiffness.

There are the following four methods for changing the stiffness of the finger mechanism[2].

- Jamming transition of powder grains
- Low melting point metal (LMPA)
- ER fluid, MR fluid
- Shape memory polymer (SMP)

First, there are examples such as J. R. Amend et al.[3] that use the jamming transition of powder grains. However, there is a problem that waterproofing is difficult because it is necessary to generate negative pressure by a vacuum pump or a compressor and an air ejector, and it is necessary for air to flow in and out.

Next, as examples of using a low melting point alloy (LMPA), there are examples such as J. Yan et al.[4], J. Shintake et al.[5], and H. Nakai et al.[6]. The tensile strength at the solid phase is large (65 MPa in the one used in this study), and it is only necessary to have a heating wire as a heat source, so it is an advantage that it can be realized compactly. But there is also the disadvantage that it takes a long time to change the stiffness.

For ER fluid and MR fluid, there are examples such as A. Pettersson et al.[7]. Among these, it has the advantage that it takes the shortest time to change the stiffness. But the yield stress is about 2 to 5 kPa for ER fluid and about 50 to 100 kPa for MR fluid[8], so it is not suitable for applications that require a large yield stress.

Finally, a shape memory polymer is also said to have weak mechanical strength like ER fluid and MR fluid.

Judging from the above, in this study, we decided to change the stiffness by using a low melting point alloy (LMPA). We aim to achieve both contact pressure distribution and concentration by incorporating a variable stiffness unit using a LMPA into the skeleton of the finger mechanism and changing the stiffness.

III. VARIABLE STIFFNESS WIRE-DRIVEN FINGER MECHANISM

The structure of the variable stiffness wire-driven finger mechanism is shown in Fig. 1. In Fig. 1 (a) is the state where all the parts including the soft skin are attached, Fig. 1 (b) is the state where only the soft skin is removed, and Fig. 1 (c) is the state where all the skeletal structures are removed.

As shown in Fig. 1 (c), the variable stiffness wire-driven finger mechanism consists of two coil springs, a continuous wire that passes through the inside of each spring, a pulley that folds the wire, and a variable stiffness unit described later in the next chapter. As shown in Fig. 1 (b), it also consists of a skeletal structure that is added between the lines of the spring and connects the two springs, the fingertip part fixed to the skeletal structure and freely rotatably connected to the pulley, and the palm part fixed to the skeletal structure on the other side. As shown in Fig. 1 (a), it also consists of a soft skin formed on the outside of the structure.

In addition to the function of the skeleton part of the soft flexible wire-driven finger mechanism that we have

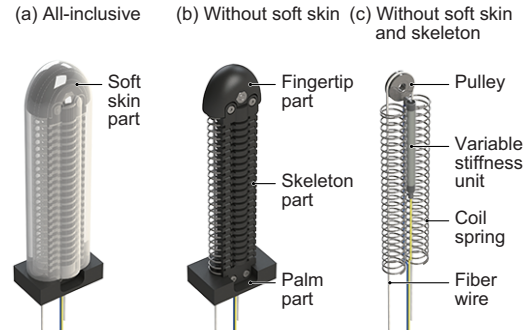


Fig. 1. Variable Stiffness Soft Waterproof Wire-driven Finger Mechanism

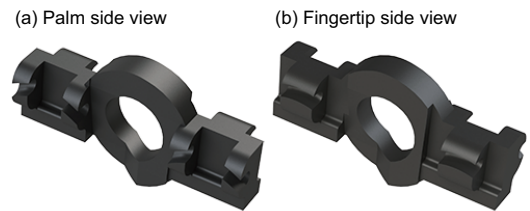


Fig. 2. Skeleton Part of Finger Mechanism

Configuration for single finger bending experiment (23 joints)

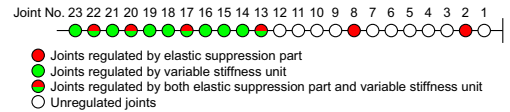


Fig. 3. Joint Configuration for Single Finger Bending Experiment

proposed[1], the skeleton part has a round hole in the center as shown in Fig. 2 so that it can hold a variable stiffness unit using a LMPA, which will be described later.

There are 23 joints in the finger mechanism used in the single finger bending experiment in the next chapter. Two stainless steel springs (Misumi, FUR12-94-A) are installed in it. The free length is 94mm, the outer diameter is 12mm, the wire diameter is 0.9mm, the pitch is 3.8mm, the spring constant is 0.17N/mm, and the material is SUS304-WPB. Flexion of the joints is limited by the elastic suppression part that we have proposed[1], and the variable stiffness unit described later as shown in Fig. 3. The number of the joint near the palm part is defined as 1.

IV. BENDING CHARACTERISTICS OF FINGER MECHANISM

The flexion characteristics of the wire-driven finger mechanism are discussed in another paper[1] and this paper describes the difference in flexion movement due to the addition of the variable stiffness unit. The difference in bending motion of the variable stiffness wire-driven finger mechanism is shown in Fig. 4. Fig. 4 (a) and (b) show the state with the soft skin removed, and Fig. 4 (c) and (d) show the state with the soft skin attached. Fig. 4 (a) and (c) show the state in which the heater is on and the stiffness of the variable stiffness unit is low. Fig. 4 (b) and (d) show the state

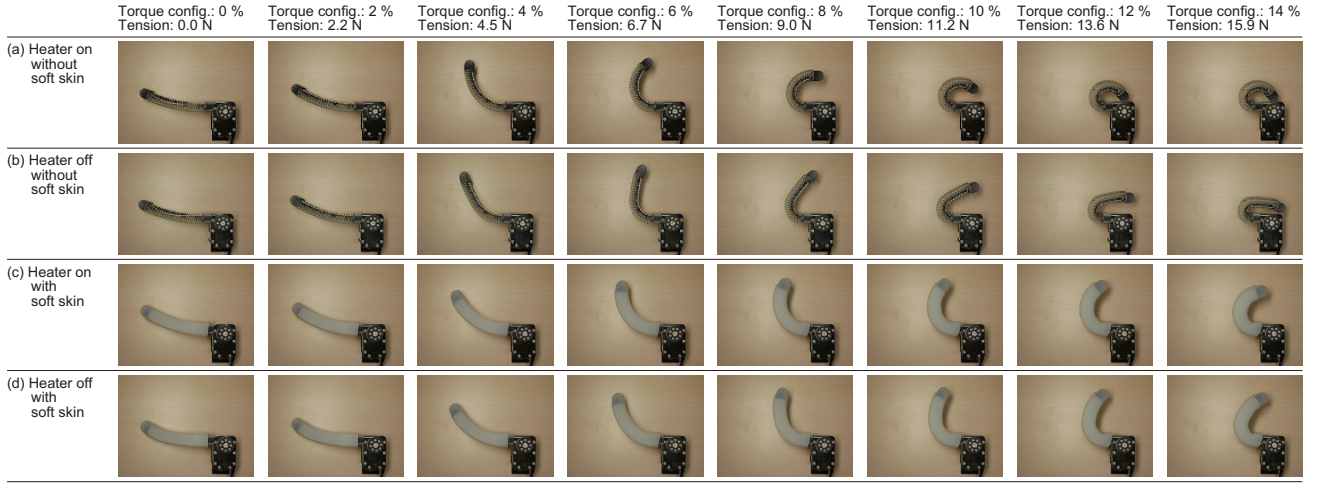


Fig. 4. Single Finger Bending Experiment of Variable Stiffness Wire-driven Finger Mechanism

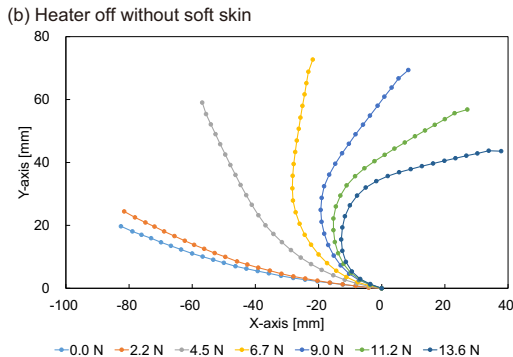
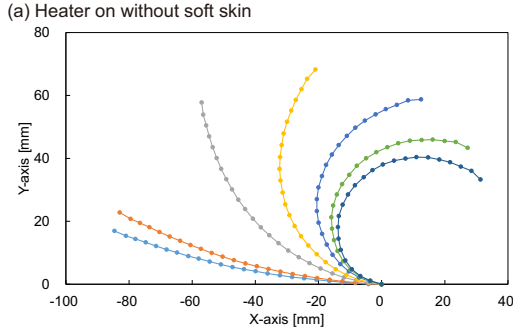


Fig. 5. Joint Position of Single Finger Bending Experiment

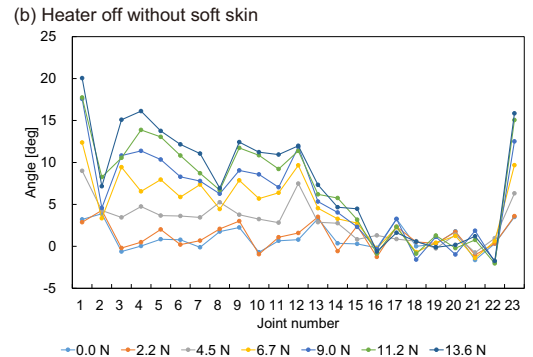
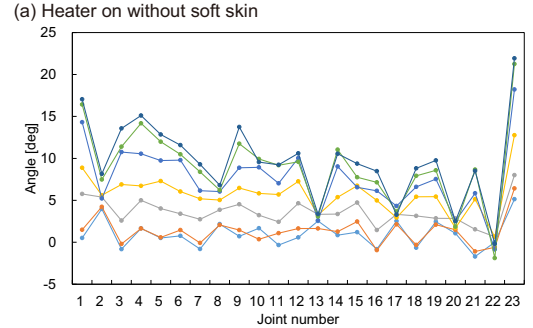


Fig. 6. Joint Angle of Single Finger Bending Experiment

in which the heater is off and the stiffness of the variable stiffness unit is high.

It is driven by the fiber wire (Hayami Industry, DB-50) connected to the pulley (diameter: 22mm), and the pulley is torque controlled by a servo motor (Robotis, Dynamixel MX-28AR). And the soft skin is molded with silicone rubber (Smooth-On, Dragon Skin FX-Pro).

As shown in Fig. 4, when the palm part is fixed and one end of the wire is pulled, rotational torque is generated between the skeleton parts and the finger mechanism bends. When the wire is loosened, the finger mechanism returns to its original state due to the restoring force of the coil springs. The soft skin follows and deforms according to bending

motion of the finger mechanism. Since it has many joints on a narrow pitch, the deformation of the soft skin is dispersed, and the concentration of local stretching and slack is small. So that the soft skin has good followability to the finger mechanism.

As shown in Fig. 4 (a) and (c), it can be seen that the entire finger is bent because the stiffness of the variable stiffness unit decreases when the heater is on. On the other hand, as shown in Fig. 4 (b) and (d), it can be seen that bending of the joints near the fingertip is restricted and only the joints near the palm is bent because the stiffness of the variable stiffness unit increases when the heater is off.



Fig. 7. Variable Stiffness Unit

When a human hand performs a motion of applying one-point pressure with a fingertip such as a pinch motion, the joints near the fingertip such as the IP joint and the DIP joint have less displacement than other joints. By switching the flexibility of the joints near the fingertip, it is possible to realize not only the distributed pressure but also the one-point pressure even with an underactuated finger.

A plot of the joint positions in the images of Fig. 4 (a) and (b) is shown in Fig. 5. The position is corrected so that the joint at the base of the finger (joint number: 1) is the origin, and the angle is corrected so that the root link is in the negative direction of the X-axis. Furthermore, Fig. 6 shows the calculated joint angles from the joint positions of Fig. 5. Regarding the joint angle, the angle at which the links are straight is set to 0, and the bending direction is set to positive.

In Fig. 6 (a), change in the joint angles of joint numbers 2, 8, 13, 17, 20 and 22 with elastic suppression parts is small, but the other joints are totally bent. In Fig. 6 (b), in addition to the joint angles of joint numbers 2, 8, 13, 17, 20 and 22 with elastic suppression parts, the joint angles of joint number 13 to 23 with a variable stiffness unit is also relatively small. As a result, it was verified that the bending characteristics can be changed by changing the stiffness of the variable stiffness unit. By changing the bending characteristics, it is possible to realize the motion of applying a distributed pressure with the entire finger when the heater is on, and the motion of applying a single point pressure with the fingertip when the heater is off.

V. VARIABLE STIFFNESS UNIT

The appearance of the variable stiffness unit is shown in Fig. 7. The variable stiffness unit encloses a LPMA in a silicone tube, and has a nichrome wire coated with a PTFE tube placed in the center to switch between the solid phase and the liquid phase of the LPMA and change the stiffness.

As shown in Fig. 8, when the heater is on and the LPMA becomes a liquid phase, the stiffness becomes low and it can be deformed by the external force applied to the tube. When the heater is off and the LPMA becomes a solid phase, the stiffness becomes high and it can't be deformed by the external force applied to the tube.

We will explain how to manufacture the variable stiffness unit. First, prepare a PTFE tube (inner diameter: 0.5mm, outer diameter: 1mm) as shown in Fig. 9 (a). Next, as shown in Fig. 9 (b), cut an aluminum round bar (material: A5056B, outer diameter: 4mm) at 4mm, make a 1mm hole in it to use it as a collar, and bond it to the PTFE tube. Furthermore,

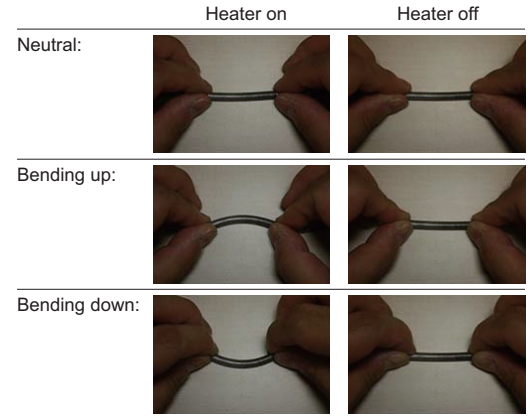


Fig. 8. Stiffness Change of Variable Stiffness Unit

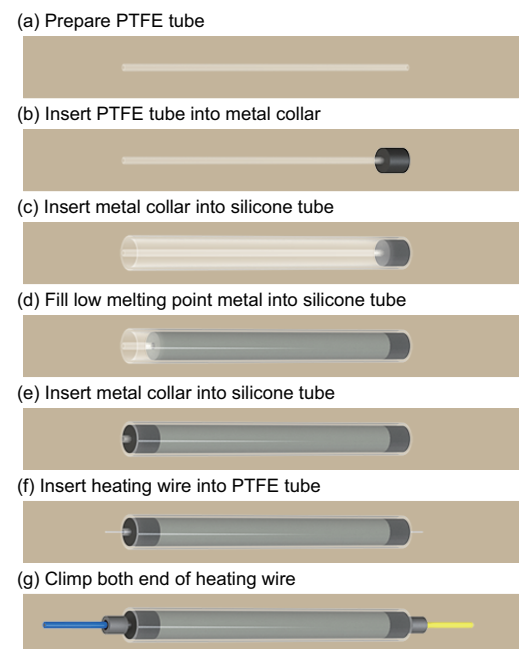


Fig. 9. Manufacturing Procedure of Variable Stiffness Unit

as shown in Fig. 9 (c), a silicone tube (inner diameter: 4mm, outer diameter: 5mm) is glued to the collar. As shown in Fig. 9 (d), a LMPA (Osaka Asahi, U-alloy 47, melting point: 47°C, tensile strength: 65MPa at 25°C) is filled in the silicone tube. At the time of filling, make the longitudinal direction of the silicone tube vertical, melt the ingot with a soldering iron to make a small mass, insert it into the silicone tube, and heat it again with a heat gun from the outside of the silicone tube to bleed air. After filling, as shown in Fig. 9 (e), the same collar used in Fig. 9 (b) is glued to the PTFE tube and silicone tube. After that, as shown in Fig. 9 (f), pass a nichrome wire (Asahi Electric, HK-NK05H, outer diameter: 0.26mm) as a heater through the PTFE tube. Finally, as shown in Fig. 9 (g), lead wires (Hitachi Metals, UL1571 (IR) LF 26AWG) are crimped to both ends of the nichrome wire with bare crimp sleeves (Nichifu, P-0.5).

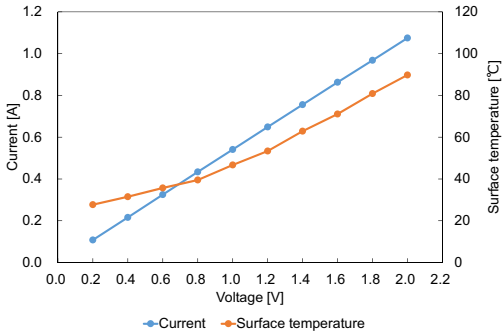


Fig. 10. Heating Characteristics of Variable Stiffness Unit

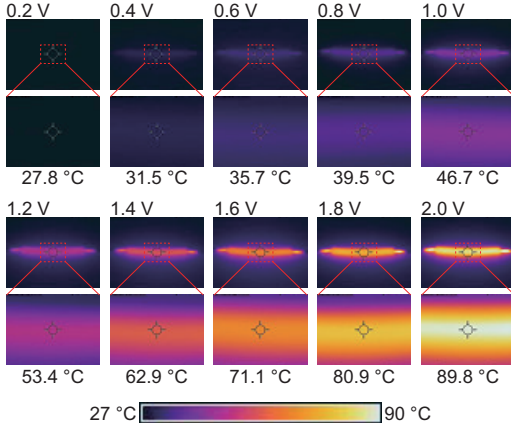


Fig. 11. Thermal Image of Variable Stiffness Unit

VI. HEATING CHARACTERISTICS OF VARIABLE STIFFNESS UNIT

We measured the heating characteristics of the variable stiffness unit. The variable stiffness unit used for the measurement was a silicone tube with a length of 50mm and a nichrome wire with a length of 70mm, as shown in Fig. 7. The current and the temperature of the silicone tube surface were measured when a voltage was applied in 0.2V increments in the range of 0.2 to 2V. The thermal camera (FLIR, FLIR i5) was used to measure the surface temperature of the silicone tube and the room temperature at the time of measurement was 27°C.

The measured voltage, current and surface temperature are shown in Fig. 10. The surface temperature image when voltage is applied is shown in Fig. 11. It was found that when the length of the nichrome wire was 70mm, the melting point of 47°C was exceeded when a voltage of 1.2V was applied. Since the current value at that time is 0.649A, the power is 0.78W. It is necessary to add 0.011W/mm when converted to 1mm of nichrome wire.

The time required for heating and cooling depends on the surrounding environment. Here we consider the case where the variable stiffness unit is alone and under a 27°C atmosphere, and the applied voltage is 1.2V. In this case, it takes about 15 minutes to exceed the melting point around 47°C when heating from 27°C at room temperature, and

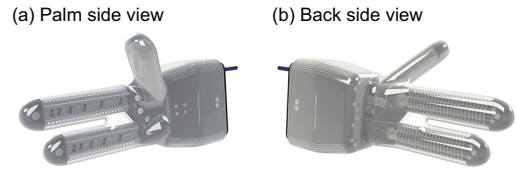


Fig. 12. Waterproof Soft Robot Hand with Soft Skin

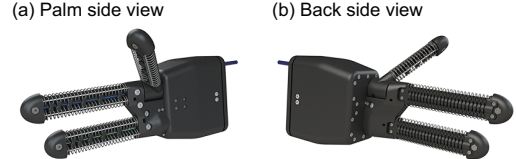


Fig. 13. Waterproof Soft Robot Hand without Soft Skin

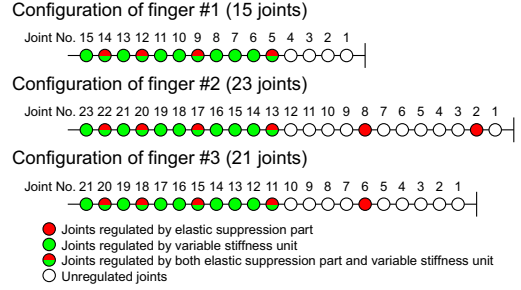


Fig. 14. Joint Configuration of Waterproof Soft Robot Hand

about 8 minutes to fall below the melting point around 47°C when cooling from 53.4°C in the steady state. To speed up heating, for example, if a voltage of 2V is applied, it takes about 3 minutes to exceed the melting point around 47°C. Therefore, by heating at a voltage of 2V for about 3 minutes and then keeping the heat at a voltage of 1.2V, the variable stiffness unit can become more practical.

VII. WATERPROOF SOFT ROBOT HAND

The appearance of the waterproof soft robot hand with the variable stiffness wire-driven finger mechanism is shown in Fig. 12 and Fig. 13. Fig. 12 shows the state including the soft skin, and Fig. 13 shows the state where the soft skin is removed.

The size of the fingers and palm of the robot hand is designed with reference to AIST Japanese hand size data[9], and is close to the standard Japanese hand size. The robot hand consists of three fingers, the first finger corresponds to the human thumb, the second finger corresponds to the human index finger and middle finger, and the third finger corresponds to the human ring finger and little finger. By integrating the roles of the index finger and middle finger, and the ring finger and little finger into one finger, the number of actuators is reduced, contributing to a compact configuration. As shown in Fig. 14, there are 15 joints on the first finger, 23 joints on the second finger, and 21 joints on the third finger. Flexion of the joints is limited by the

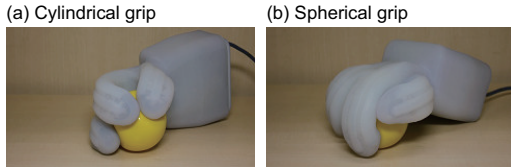


Fig. 15. Cylindrical and Spherical Grip of Waterproof Soft Robot Hand

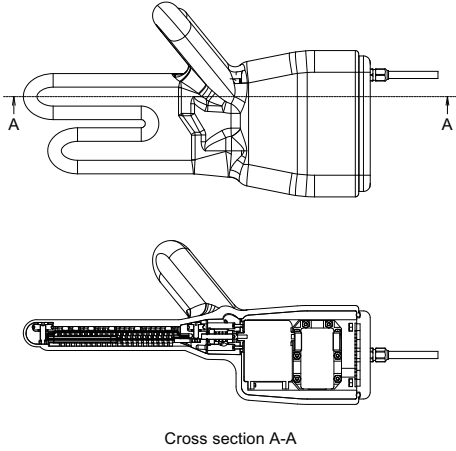


Fig. 16. Cross-sectional View of Waterproof Soft Robot Hand

elastic suppression part[1] and the variable stiffness unit. The arrangement of the variable stiffness unit is determined experimentally so that the three fingertips are aligned when the LMPA becomes a solid phase without energizing the heater.

The first finger, which corresponds to the thumb, has a structure that allows abduction and adduction. By providing a pulley that regulates the wire path on the same axis as the rotation axis of abduction and adduction, the change of the wire path is small. The soft robot hand[1], which has been proposed so far, can only grip objects by a cylindrical grip with the fingers facing each other as shown in Fig. 15 (a). But the waterproof soft robot hand in this paper can grip objects by not only a cylindrical grip but also a spherical grip with the fingers not facing each other as shown in Fig. 15 (b).

The entire robot hand is covered with an integrated soft skin made of silicone rubber. A part of the palm has a structure in which the skeletal structures of the second and third fingers are connected by the integrated soft skin, and this part is actively deformed like the wire-driven fingers. As shown in the cross-sectional view of Fig. 16, the edge of the integrated soft skin is pressed by a grooved plate to make the robot hand waterproof.

In order to make an integrated soft skin of a waterproof soft robot hand, silicone rubber (Smooth-On, Dragon Skin FX-Pro) was molded in the desktop vacuum casting machine (Ideatube, Swing Cast) with 15 mold parts made with 3D printers shown in Fig. 17.

The system configuration of the waterproof soft robot hand is shown in Fig. 18. Four servo motors (Robotis, Dynamixel MX-28AR) for bending three fingers, and abduction and

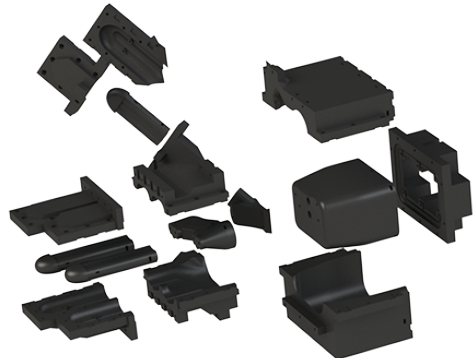


Fig. 17. Mold Parts for Integrated Soft Skin of Waterproof Soft Robot Hand

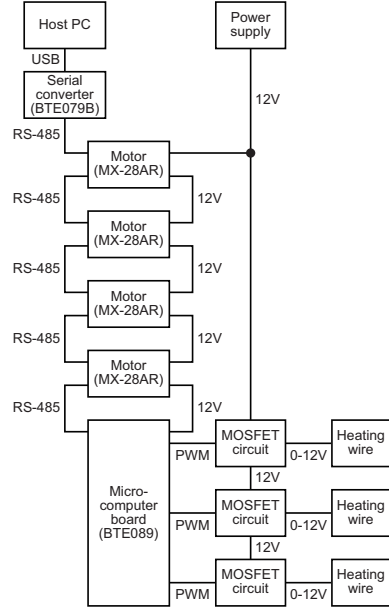


Fig. 18. System Configuration of Waterproof Soft Robot Hand

adduction of the first finger are daisy-chained by RS-485. And they are connected to the host PC through a serial converter of USB and RS-485. The microcomputer board for heating wire control (Best Technology, BTE089) is also daisy-chained by RS-485, and the voltage applied to the heater is controlled by switching the MOSFET circuit using the PWM signal output from the microcomputer board.

VIII. PIPE GRASPING AND PINCHING EXPERIMENT

In order to observe the motion of the waterproof soft robot hand when grasping and pinching, we conducted an experiment of grasping and pinching a pipe. An acrylic pipe with an outer diameter of 70mm, a thickness of 3mm, and a length of 300mm was used as the object. A sensor sheet (Tekscan, I-Scan System with Pressure Mapping Sensor 5211 (pressure range: 80kPa)) was wrapped around the surface of the pipe and the contact pressure distribution was measured at 100 Hz. The state of contact with the pipe and the

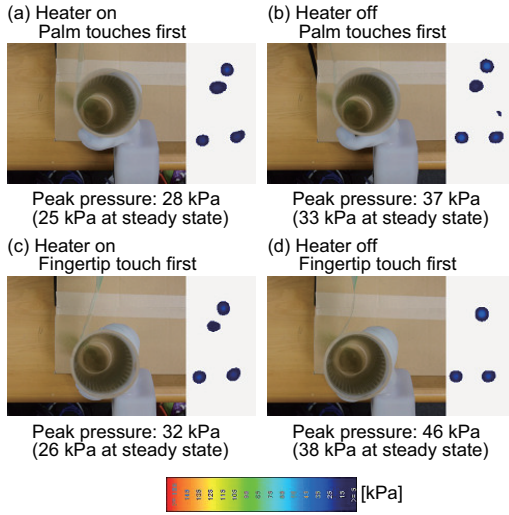


Fig. 19. Results of Pipe Grasping and Pinching Experiment

result of contact pressure distribution are shown in Fig. 19. Experiments were conducted with the torque limit set to 60 % and the wire tension is constant at 75.2N. And the contact pressure distribution shown in Fig. 19 is the data of the steady state where the gripping state is stable after 9.5 seconds have passed since the gripping motion started.

In order to realize the gripping motion, it is necessary for the pipe and the robot hand to be in the relative position where the pipe comes into contact with the palm first. In this case, the contact area is larger and the peak contact pressure is smaller when the heater is energized than when it is not energized as shown in Fig. 19 (a) and (b). It can be seen that it is better to energize the heater in order to disperse the contact pressure.

On the other hand, in order to realize the pinching motion, it is necessary for the pipe and the robot hand to be in the relative position where the pipe comes into contact with the fingertips first. In this case, when the heater is energized, the pipe is pulled toward the palm as force is applied and finally the pipe is in contact with the palm in a steady state as shown in Fig. 19 (c). This steady state is similar to the steady state of grasping motion. When the heater is not energized, the movement of the pipe being drawn to the palm is alleviated and the force can be generated only at the fingertips as shown in Fig. 19 (d). The peak contact pressure is also larger than that when the heater is not energized, and it can be seen that it is better not to energize the heater in order to concentrate the contact pressure.

From the above, it is possible to achieve both distribution and concentration of contact pressure by causing a phase change of the LPMA depending on the energization status of the heater.

IX. MASSAGE EXPERIMENT BY REMOTE CONTROL OF DUAL-ARM ROBOT

A massage experiment was conducted using the developed waterproof soft robot hand. Using the dual-arm robot

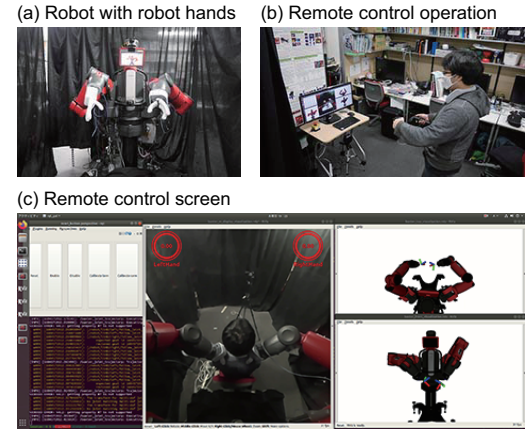


Fig. 20. Settings of Remote Control Experiment



Fig. 21. Massage Experiment by Remote Control of Dual-arm Robot

(Rethink Robotics, Baxter), the waterproof soft robot hand developed in this paper was attached to the right arm, and the soft robot hand developed in the past paper[1] was attached to the left arm. The left robot hand is used in the hair washing experiment of the next chapter. This research involving human subjects was approved by the research ethics review board of Graduate School of Information Science and Technology, The University of Tokyo on December 18, 2020.

The operation of the robot arm and robot hands is performed by remote control, and the operator is presented with the transmitted video captured by the fisheye camera (Kodak, PIXPRO 4K SP360) and a 3D model of the robot as shown in Fig. 20 (c). When the operator holds the controllers (HTC, VIVE) in both hands and moves them as shown in Fig. 20 (b), the target position and posture of the robot hands on the 3D model changes according to the position and posture of the controllers, and the actual robot operates to follow the trajectory[10].

The massage experiment was performed on the following four motions.

- Forearm massage (cylindrical surface, small radius)
- Shoulder massage (cylindrical surface, large radius)
- Hand massage (flat surface, both sides)
- Back massage (flat surface, one side)

Fig. 21 (a) shows the motion of massaging the forearm. In

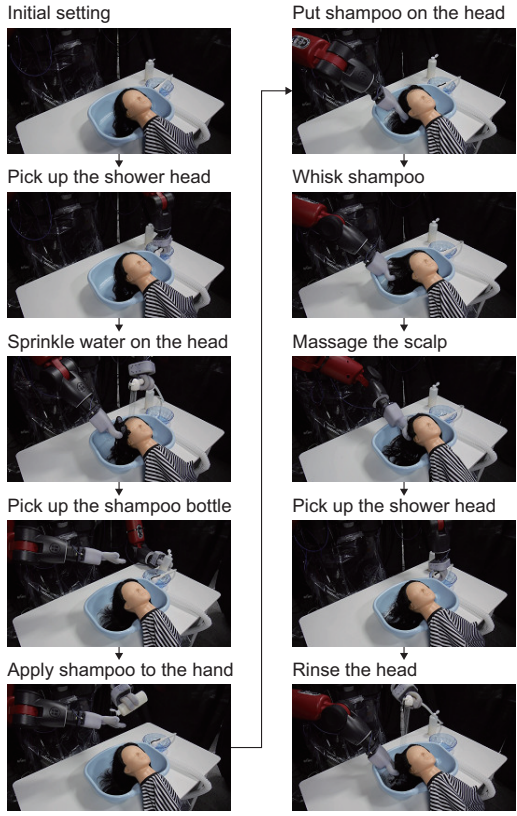


Fig. 22. Hair Washing Experiment by Remote Control of Dual-arm Robot

this motion, it is necessary to distribute the contact pressure, so the heater wires were turned on and the fingers could be freely deformed. As a result, it was found that the pressure could be distributed by wrapping the arm. Fig. 21 (b), (c) and (d) shows the motion of massaging the shoulder, the hand and the back. In these motions, it is necessary to concentrate the contact pressure, so the heater wires were turned off and the fingers were restricted in deformation. As a result, it was found that the pressure could be concentrated at one point without increasing the shearing force.

From the above experiments, it was confirmed that not only the pressure distribution but also the pressure concentration can be realized by changing the stiffness of the variable stiffness unit.

X. HAIR WASHING EXPERIMENT BY REMOTE CONTROL OF DUAL-ARM ROBOT

A hair washing experiment was performed using the developed waterproof soft robot hand. The experimental environment is the same as the previous massage experiment. Fig. 22 shows the motion of washing hair. In these motion, it is necessary to concentrate the contact pressure, so the heater wires were turned off and the fingers were restricted in deformation.

First of all, the robot grasps the shower head with the left hand, moves it to the head, turns on the water, and spreads water by moving the right hand along the head. Next, the robot grasps the shampoo bottle with the left hand, moves it

over the right hand, and then puts shampoo on the palm of the right hand. The robot spreads the shampoo on the head with the shampoo on the right palm and move the fingers to whisk the shampoo. After that, the robot massages the scalp with the fingertips of the right hand. Finally, the robot grasps the shower head with the left hand, moves it to the head, turns on the water, and rinses hair with water by moving the right hand along the head.

From the above experiments, it was confirmed that a series of hair-washing actions can be realized by using the developed waterproof soft robot hand. It was also confirmed that the waterproof property of the soft skin is also functioning.

XI. CONCLUSION

In this paper, we proposed the variable stiffness soft finger mechanism equipped with the various stiffness unit using a low melting point alloy (LMPA), and evaluated its bending characteristics. We also developed a waterproof soft robot hand equipped with the finger mechanism, and conducted a pipe grasping and pinching experiment and a remote control experiment of massage and hair washing. By changing the stiffness, it was confirmed that not only the gripping motion and massage motion that distribute the contact pressure but also the pinch motion and acupressure motion that concentrate the contact pressure are possible. The waterproof performance by the soft skin was also confirmed. As a future prospect, we plan to evaluate the physiological and psychological effects on the human body.

REFERENCES

- [1] T. Hirose, Y. Kakiuchi, K. Okada, and M. Inaba. Design of soft flexible wire-driven finger mechanism for contact pressure distribution. In *2019 IEEE/RSJ International Conference on Intelligent Robots and Systems (IROS)*, pp. 4699–4705, Nov 2019.
- [2] J. Shintake, V. Cacucciolo, D. Floreano, and H. Shea. Soft robotic grippers. *Advanced Materials*, Vol. 30, No. 29, p. 1707035, 2018.
- [3] J. R. Amend, E. Brown, N. Rodenberg, H. M. Jaeger, and H. Lipson. A positive pressure universal gripper based on the jamming of granular material. *IEEE Transactions on Robotics*, Vol. 28, No. 2, pp. 341–350, April 2012.
- [4] J. Yan, H. Zhang, P. Shi, X. Zhang, and J. Zhao. Design and fabrication of a variable stiffness soft pneumatic humanoid finger actuator. In *2018 IEEE International Conference on Information and Automation (ICIA)*, pp. 1174–1179, Aug 2018.
- [5] J. Shintake, B. Schubert, S. Rosset, H. Shea, and D. Floreano. Variable stiffness actuator for soft robotics using dielectric elastomer and low-melting-point alloy. In *2015 IEEE/RSJ International Conference on Intelligent Robots and Systems (IROS)*, pp. 1097–1102, Sep. 2015.
- [6] H. Nakai, Y. Kuniyoshi, M. Inaba, and H. Inoue. Metamorphic robot made of low melting point alloy. In *IEEE/RSJ International Conference on Intelligent Robots and Systems*, Vol. 2, pp. 2025–2030 vol.2, Sep. 2002.
- [7] A. Pettersson, S. Davis, J.O. Gray, T.J. Dodd, and T. Ohlsson. Design of a magnetorheological robot gripper for handling of delicate food products with varying shapes. *Journal of Food Engineering*, Vol. 98, No. 3, pp. 332 – 338, 2010.
- [8] K. Hiwatari. Vibration control of building structures utilizing semi-active damper. *Kobe University Thesis or Dissertation*.
- [9] M. Kouchi. AIST Japanese hand dimensional data, 2012. <https://www.airc.aist.go.jp/dhrt/hand/index.html>.
- [10] S. Kitagawa, T. Hirose, K. Shinjo, K. Okada, and M. Inaba. Audio-visual integrated remote manipulation system using robot with soft hand. In *21th SICE System Integration Division Annual Conference*, 2020.